ARTICLES

Mechanics of the kinesin step

N. J. Carter[1] & R. A. Cross[1]

Kinesin is a molecular walking machine that organizes cells by hauling packets of components directionally along microtubules. The physical mechanism that impels directional stepping is uncertain. We show here that, under very high backward loads, the intrinsic directional bias in kinesin stepping can be reversed such that the motor walks sustainedly backwards in a previously undescribed mode of ATP-dependent backward processivity. We find that both forward and backward 8-nm steps occur on the microsecond timescale and that both occur without mechanical substeps on this timescale. The data suggest an underlying mechanism in which, once ATP has bound to the microtubule-attached head, the other head undergoes a diffusional search for its next site, the outcome of which can be biased by an applied load.

Recent single-molecule work on the kinesins-1 firmly supports a model in which the motor walks along, using alternate microtubule-binding heads as holdfasts[1–3]. The step size is 8 nm, corresponding to the axial distance between microtubule heterodimer subunits, and is independent of ATP concentration and load[4,5]. There are reports of mechanical substeps[6,7]. Stepping is tightly coupled to ATP turnover: a step does not require the binding of two ATPs[8,9] and one ATP molecule is consumed on average per step[10], except possibly at high load[11].

During the long dwell intervals between steps at limiting ATP concentrations, kinesin is paused, waiting for ATP to bind. Kinesin in this waiting state is tightly attached to the microtubule by its nucleotide-free trailing (holdfast) head, whereas its ADP-containing leading (tethered) head is stably inhibited from undergoing microtubule-activated ADP release[12]. ATP binding to the holdfast head relieves this inhibition and allows the microtubule-activated release of ADP from the other head[12]. A similar scheme is thought to operate under load, such that each forward mechanical step reports the commitment of an ATP molecule to the chemical cycle[13].

Although these broad features of the mechano-chemical cycle are clear, the physical mechanism by which the motor transfers between microtubule binding sites, thereby exchanging the load from one head to the other, remains uncertain. Two different sorts of scheme have been proposed. In lever arm models, the motor head attaches tightly to the track and concomitantly or subsequently undergoes a large shift in its shape or tilt angle. The motion imparted by this conformational change can be amplified by a lever arm rigidly attached to the moving part of the motor head. Some myosins use this kind of mechanism, as evinced by a recent demonstration that the lever arm of myosin Ie could be re-engineered to harness the same conformational change to drive reverse-directed motion[14]. Recent evidence from muscle fibres confirms that the myosin II lever arm drives muscle contraction and indicates that the lever throw is dependent on load[15]. For kinesin, the neck linker model proposed by Rice *et al.*[16] is a kind of lever arm model, in which ATP-dependent docking of the flexible neck linker against the head acts like a lever arm to shift the load along the microtubule axis. A contrasting type of model emphasizes the diffusional search made by the head for its next binding site[17,18]. The motor diffuses randomly along its track, stretching a spring somewhere in its structure, and large diffusional excursions in the progress direction are selectively captured by the track-binding event. In the pure form of this kind of model, the conformational change accompanying track binding serves to stabilize binding but does not significantly stretch the spring.

The mechanism of each kinesin step could consist of elements of both processes (diffusion-to-capture plus a conformational change). Detailed information about the amplitude, time course and reversibility of stepping can help to sort out the contributions of each process. To examine stepping in more detail we used the now-classical single-bead optical-trap arrangement in which a single molecule of kinesin is attached to a spherical bead about 1 μm in diameter. The bead is optically trapped at the focus of an infrared laser[19] and the trap is steered so as to bring the kinesin within range of an immobilized microtubule. The kinesin then walks along the microtubule, tending to pull the bead out of the trap, while the trap applies an opposing force tending to restore the bead to the trap centre. Within the range of interest, the trap acts like a spring obeying Hooke's law. By accurately tracking the bead, the stepwise motions of the attached kinesin molecule can be observed. We measured in particular the effect of extreme backward loads on the pattern of stepping, and we applied a step-averaging algorithm that provides improved spatiotemporal resolution, allowing us to search for substructure within averaged 8-nm steps.

High backward loads induce processive backward stepping

At saturating ATP concentrations, when the stepping rate is not limited by the rate of ATP binding, the velocity of kinesin varies roughly linearly with force until the motor is stepping close to stall[5,20–22], at which point backward steps become more frequent (we will call steps taken towards the microtubule plus end forward steps, and steps towards the minus end backward steps). One view is that such backward steps are slippage events. Slippages and detachments certainly occur; however, it has recently been reported that the probability of single backward steps depends on the ATP concentration[17], implying that backward steps have a definite mechanism that is triggered by ATP binding, as do forward steps.

We explored the effects of substantial backward and forward loads on stepping (Fig. 1). Record 2 shows that if, during a run of processive forward steps, the load is suddenly increased to super-stall levels, kinesin can respond by stepping processively backwards until stall re-establishes. The figure shows processive runs of backward steps from 14 pN of backward force down to stall at 7 pN. At high loads, detachments are frequent, but by considering only steps that occurred within a chain of consecutive steps we were able to determine the mechanical behaviour over the entire operational range of loads.

[1]Molecular Motors Group, Marie Curie Research Institute, The Chart, Oxted, Surrey RH8 0TL, UK.

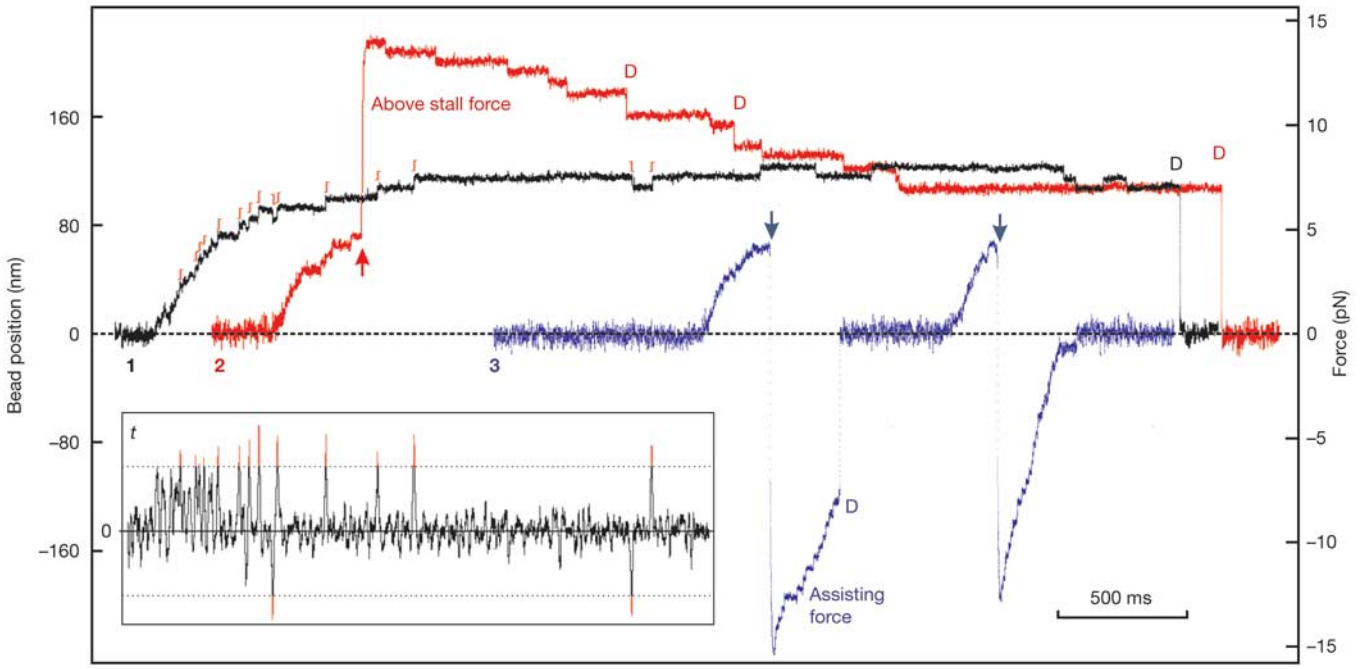

Figure 1 | Example optical trapping records. Three superimposed records showing the movement of single kinesin molecules towards stall force, over time. In record 1 (black), the trap and microtubule remain fixed throughout, and the kinesin walks with 8-nm steps away from the trap centre (dashed line) to stall force and finally detaches. In record 2 (red), on reaching 4 pN the microtubule is moved rapidly (upward arrow), pulling the kinesin to about 14 pN force. In some instances the kinesin responds with processive backward steps to stall force (7–8 pN). More commonly at forces above 10 pN, the kinesin would detach after a few or no backward steps, the bead returning to trap centre. Record 3 (blue) shows the opposite procedure. On reaching the 4-pN trigger force, the microtubule is quickly moved (downward arrows) to apply a large negative (assisting) force to the kinesin. Two successive experiments on the same molecule are shown. For automated dwell time calculations and step-averaging, a *t*-test step finder was applied to the bead position data. The inset shows the *t*-test profile for the first part of record 1. Steps are defined where the *t*-value exceeds a preset threshold value (dotted line). The located steps are shown offset just above record 1. In all records, detachment events (steps larger than 12 nm recognized by the step finder) are marked with D. Conditions: single kinesin molecules on 560-nm polystyrene beads, 1 mM ATP. The trap stiffnesses for the beads in these records were 0.064, 0.067 and 0.064 pN nm^{-1}, respectively. The force scale represents a trap stiffness of 0.065 pN nm^{-1}. Stage movements (arrows) were typically complete within 200 ms. The data shown are 1-ms boxcar filtered.

To do this we used an automatic algorithm (see Methods) to find steps within a data set of multiple records, and to determine the dwell time (the time interval between the previous step and the current step) and amplitude (the distance moved) for each step. Figure 2a shows the incidence and the amplitude of forward and backward steps over the range −15 pN (assisting load) to +15 pN (inhibitory load). The inset shows that the ratio of the number of forward steps to the number of backward steps at any particular load depends exponentially on the load. At the stall force of 7.2 pN (ref. 17) this ratio is 1. The stall force does not seem to depend on the ATP concentration, because the choice between forward and backward stepping depends only on load, not on ATP concentration.

Figure 2b plots the variation of dwell time with load for forward and backward steps. At all loads, the dwell time for both forward and backward steps decreases as the ATP concentration is increased, confirming that ATP binding is required for both forward and backward steps[17]. Under forward (assisting) loads (in the range −2 to −15 pN in Fig. 2b) only forward steps are observed, and their dwell time depends only on the ATP concentration, not on the load, indicating that a chemical step (ATP binding) is limiting. Under backward load, the dwell time for forward steps depends exponentially on the load, as expected for a particle diffusing over an activation energy barrier in accordance with Kramers theory[23–25]. The load–dwell-time curve for forward steps is exponential above about 3 pN both at 1 mM ATP and at 10 μM ATP, and the exponents are similar at high and low ATP concentrations, which is consistent with a single, common, rate-limiting mechanical step under high backward load at both high and low ATP. At any particular backward load, dwell times are exponentially distributed (Supplementary Fig. S2).

Above stall force, backward steps predominate. Their dwell times depend on the ATP concentration, confirming that backward steps, like forward steps, are triggered by ATP binding. It has been reported[17] that the mean dwell time for single backward steps is load-independent. We confirm their conclusion and extend it to include processive backward stepping under super-stall loads of up to 15 pN. Figure 2c plots force–velocity curves calculated by dividing the mean step size (forward steps positive, backward steps negative) by the mean dwell times shown in Fig. 2b.

Steps are microsecond events with no substeps

There are two reports of substeps in the literature[7,26], and several current models for the kinesin mechanism predict that the 8-nm step consists of two or more mechanical substeps, with more than one biochemical kinetic step occurring during an 8-nm physical step. To search for mechanical substeps we attached kinesin to smaller beads, to give an improved temporal response[7], and used a step-averaging algorithm to increase spatial resolution. Our algorithm automatically finds steps and then does a global fit to find the best single-exponential fit across the full data set of steps (see Methods). The origins of these fits are then used to synchronize the raw data records for the steps so that they can be ensemble averaged. We found that the resulting average step was a simple monophasic event; no mechanical substeps were detectable (Fig. 3) either before or during the major event.

To test the limits of detection in our system we generated synthetic data by adding substeps of defined amplitude and duration to real, recorded noise. The simulations (Supplementary Information) show that a bead position substep lasting more than 30 μs would be necessary to increase the averaged bead rise time detectably beyond

that which we observe. Our data therefore rule out substeps of duration more than 30 μs.

Figure 3 shows that the time constants for the ensemble averaged forward and backward steps are very similar. Steps were faster if we used slightly smaller beads, which diffuse more rapidly (Fig. 3).

Model

That the forward directional bias in kinesin can be reversed by pulling backwards on the motor suggests that the tethered head makes a diffusional search for its next site, the outcome of which can be biased by an applied load.

System stiffness (trap stiffness plus bead–kinesin–microtubule link stiffnesses) in our experiments increases from about 0.06 pN nm^{-1} (trap stiffness) to more than 0.65 pN nm^{-1} during force production. All the various links in the system will contribute series compliances, but we can nevertheless use the measured stiffness at high load to set a lower limit of 0.6 pN nm^{-1} on kinesin head stiffness. This low limit for the head stiffness is consistent with a diffusional mechanism (diffusion through 8 nm followed by capture) because at zero load the Kramers time[25] for a protein of 5 nm radius to diffuse 8 nm is 7 μs. The Kramers time rises to 8 ms at a 1.7 pN nm^{-1} kinesin head stiffness, which sets an upper limit on head stiffness for a diffusional mechanism.

The absence of substeps within the 8-nm kinesin step indicates that load transfers from one head to the other in a single mechanical event. As previously discussed, we envisage that forward steps and backward steps begin from a common intermediate (the parked state; Fig. 4), in which the trailing head lacks nucleotide and acts as a holdfast to the microtubule, while the ADP-containing tethered head is unbound and unloaded[12,27]. ATP binding to the holdfast head acts as a gate that allows the tethered head to begin a diffusional search for its next binding site. Ordinarily the ensuing search pattern is biased towards the microtubule plus end. This might be achieved by having the holdfast head guiding the binding direction of its partner. The neck linker docking scheme proposed by Rice and colleagues[16] has this property, but is ruled out in its original form on several grounds[28], and particularly because neck linker docking does not have enough energy associated with it to drive stepping at high loads[29]. Nevertheless, an ATP-dependent parking and unparking of the tethered head in a forward-biased position remains in our view highly plausible, albeit in our model ATP unparks the tethered head rather than parks it. Once the tethered head locates an empty site on the microtubule, strain-dependent, microtubule-activated ADP release occurs, converting the newly attached head to strong microtubule binding and transferring the load stably to it. In the model there is a transient two-heads-attached state, but the load is always born on one head only. Backwards mechanical strain counteracts the intrinsic forward bias in the diffusional search, thus increasing the probability that the tethered head will bind behind the holdfast head. For a backward step, the newly bound tethered head is unloaded as it undergoes microtubule-activated ADP release. Consistent with this is our observation that the dwell time for backward steps at high backward loads depends on the ATP concentration but not on the load.

Comparison with other models

Competing models for the kinesin mechanism agree that a decrease in efficiency occurs close to stall, due either to futile cycles[30] or to ATP-driven backward steps[24]. In our model, tight coupling of stepping to ATP binding is retained under all conditions, but the

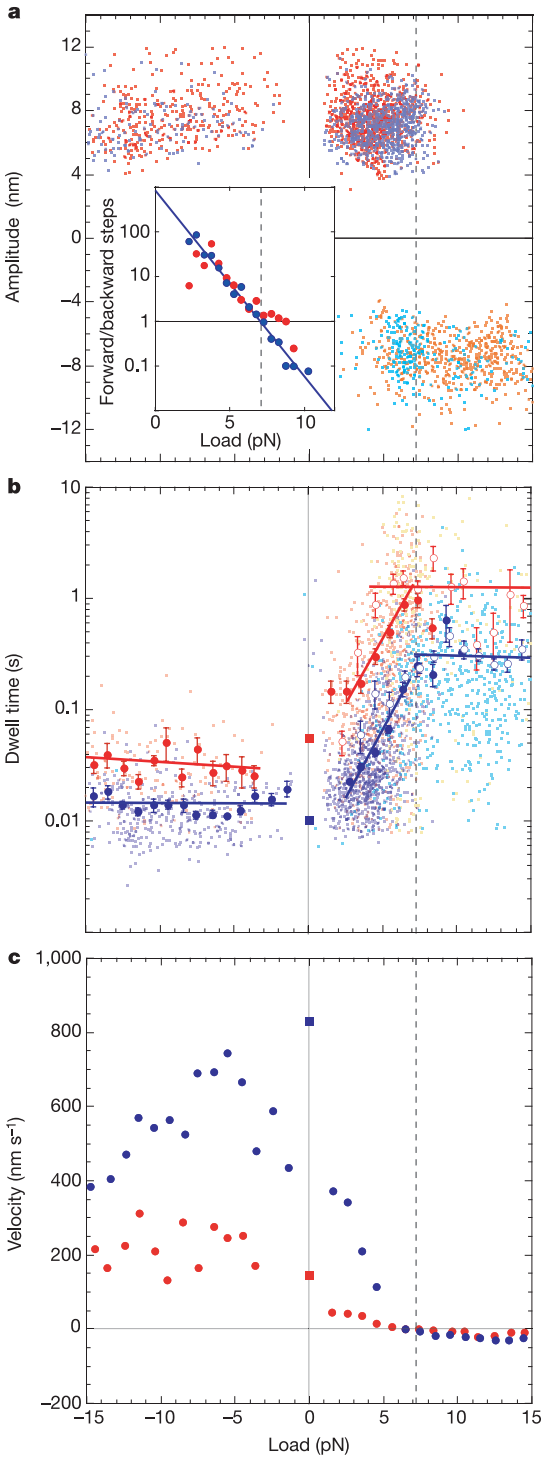

Figure 2 | Stepping behaviour. **a**, Plot of step amplitudes against load. Data for 1 mM ATP: forward steps in blue, backward steps in cyan. Data for 10 μM ATP: forward steps in red, backward steps in orange. Forward and backward steps have equal mean amplitudes. Inset, ratio of forward to backward steps plotted against the load; data for 1 mM ATP are shown in blue, and for 10 μM ATP in red. The fit is: ratio = $802e^{-0.95 \times \text{load}}$, with the load in piconewtons. **b**, Plot of dwell times against load. Data were binned with 1-pN intervals, and the mean dwell and s.e.m. were calculated for each bin. The colour key is as in **a**; filled circles are mean forward step dwells, open circles are mean backward step dwells. Mean dwell data for forward steps above 3 pN were fitted to single exponentials (solid lines). The fits are dwell = $0.0036e^{0.57 \times \text{load}}$ at 1 mM ATP and dwell = $0.0256e^{0.55 \times \text{load}}$ at 10 μM ATP, with the load in piconewtons. Other fits are by linear regression over the ranges shown by the solid lines. In the region 5–8 pN the dwell time distribution for backward steps is distorted slightly by the occurrence of forward steps, and vice versa (see Methods). **c**, Force–velocity curve. Velocities were calculated as mean amplitude divided by mean dwell time for each bin, taking the bins and the mean dwell times from **b**. Red data, 10 μM ATP; blue data, 1 mM ATP. The zero-load data (squares) are calculated from the bead velocities observed with the trap turned off.

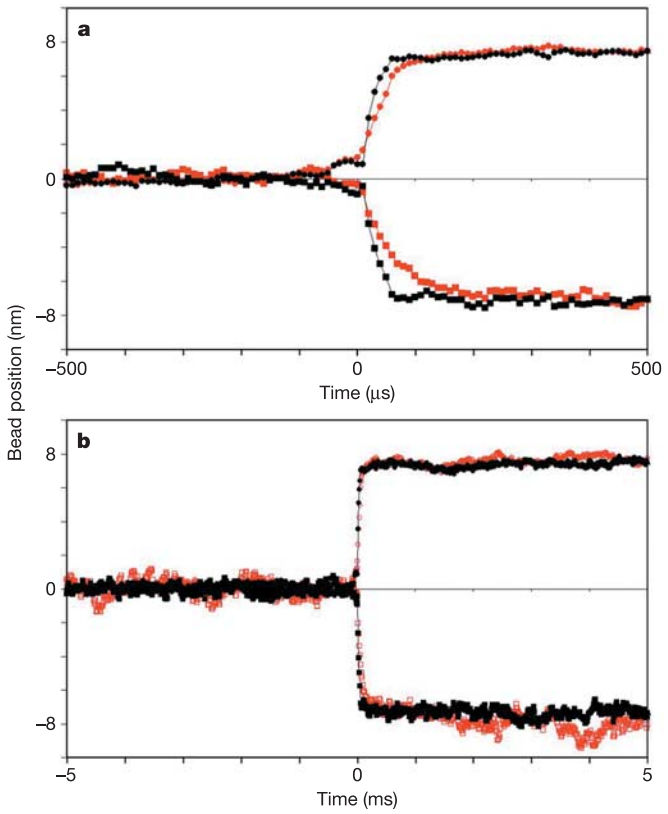

Figure 3 | Average time course of forward and backward steps. **a**, **b**, The same data sets are shown on two timescales: fine (**a**) and coarse (**b**). Step positions were determined automatically with a *t*-test step finder, followed by a least-squares exponential fit for step position refinement. The averaged forward steps (circles) and backward steps (squares) for two bead sizes are shown: the fit time constant for 500-nm beads (black) was faster than that for 800-nm beads (red). For 500-nm beads, forward steps ($n = 1{,}693$) had time constant 15.3 μs, amplitude 7.39 nm and average force 5.0 pN; for backward steps ($n = 316$) these were 19.4 μs, 7.34 nm and 6.1 pN, respectively. For 800-nm beads, forward steps ($n = 565$) had time constant 35.9 μs, amplitude 7.6 nm and force 4.7 pN; for backward steps ($n = 68$) these were 37.3 μs, 7.8 nm and 5.6 pN, respectively. All records used for the step averaging were recorded at 1 mM ATP.

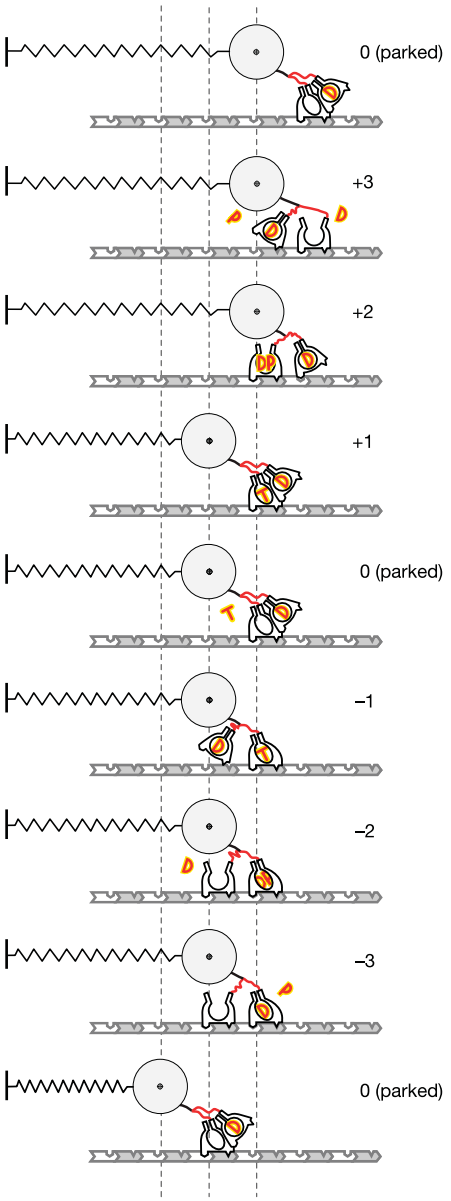

Figure 4 | Model. Before ATP binding, the motor is parked (state 0): the holdfast head remains stably bound to the microtubule and the ADP-containing tethered head cannot access its new site. Straining this state either forwards or backwards does not induce stepping. ATP (T) binding to the holdfast head sanctions ADP (D) release from the tethered head. Forward steps (+1, +2, +3, 0) occur when the tethered head binds in front of the holdfast head, backward steps (−1, −2, −3, 0) when it binds behind. The choice between forward and backward stepping depends on the applied load (the spring). In the figure, the central state 0 represents stall, in which the backward load applied by the trap (represented by the stretched spring) is such that the tethered head has an equal probability of stepping forwards or backwards. To make a forward step, the motor needs to make a diffusional excursion in the progress direction. This excursion can then be locked in by irreversible ADP release from the lead head.

probability of a forward step decreases exponentially with increasing load, whereas the probability of a backward step is constant. At stall, the probability of forward stepping is equal to that of backward stepping. Above stall, our model predicts that efficiency goes negative as backward steps begin to predominate. Note, however, that although we know that backward stepping requires ATP binding, there is at present no evidence that backward stepping is coupled to ATP turnover.

There are previous reports of substeps[6,7], and several current models predict substeps[30–32]. Our data rule out substeps that take longer than 30 μs. This indicates that the appearance of substantial substeps in previous analyses might have been an artefact. The current data gainsay models in which kinesin steps along the 4-nm tubulin monomer repeat in microtubules. Similarly, our data argue against models that predict substeps arising from rapidly equilibrating mechanical substates[30]. The data support one-stroke models[33] and specifically exclude models that forbid backward steps. Models in which backward stepping synthesizes ATP[31] are unlikely, because they predict that the frequency of backward steps should decrease at high ATP concentration, whereas we observed the opposite.

Our proposed model for processive kinesins bears striking similarities to the classical Huxley scheme for myosin[34], in that in both cases the motor head diffuses into a highly strained state, locks on to the track and then detaches at a strain-dependent rate. For myosin, this original scheme proved inadequate to account for the mechanical behaviour and was modified to include multiple bound mechanical states linked by strain-dependent conformational changes[35]. For processive kinesins, a model with biased diffusion to capture followed by a single, strain-dependent conformational change coupled to ADP release seems adequate. It will now be

important to determine how the current data on the mechanism of kinesin processivity relate to the mechanisms of non-processive kinesins and of minus-end-directed kinesins.

METHODS

Sample preparation. Experiments used BRB80 plus 5 mM dithiothreitol and a glucose oxidase/catalase oxygen-scavenging system. Polystyrene beads (500, 560 and 800 nm; Polysciences) were incubated with 0.2 mg ml^{-1} casein and decreasing concentrations of full-length *Drosophila* kinesin[10]. We used bead populations in which most beads were not motile, ensuring that the vast majority of motility observed was single molecule. Pig brain microtubules were adsorbed directly on sonicator-cleaned coverslips. Each buffer contained the desired final ATP concentration (1 mM or 10 μM) to avoid any ATP dilution by mixing in the flow cell. All recordings were made at 23 °C.

Transient two-dimensional force-feedback. In some records, once the kinesin had reached a 4-pN trigger point, the motor was pulled to a large predefined positive or negative force by moving the microtubule (piezoelectric stage) in the direction of the plus or minus end. The transient software-based force-feedback uses both on-axis and off-axis bead position data, taking into account both trap stiffness and microtubule orientation and polarity. Typically, microtubule movement was complete within 200 ms, after which the feedback was switched off and the trap and stage positions were fixed.

Bead position measurement. The quadrant photodiode detector, amplifier and sampling circuitry had a combined bandwidth of 46 kHz (−3 dB position) and was free of gain-peaking. The rise time was measured at just less than 10 μs (signal equivalent to 10 nm for a 560-nm bead). The system achieves high bandwidth at the cost of increased positional noise (root-mean-square noise is equivalent to 2.1 nm of movement of the 560-nm beads, measured at 100 kHz without sample averaging). Most data were sampled at 80 kHz (per channel) and averaged down to 20 kHz for storage and analysis. A subset of the data used in the fast step averaging were sampled at 100 kHz and stored without sample averaging. With the 560-nm beads, the position detector was linear (less than 5% attenuation) over a range that extended half a bead radius on each side of the quadrant centre. For each recording, once a particular microtubule orientation and polarity had been established, the trap position was offset to provide the maximum linear range from the position detector.

Step finder algorithm: dwell times and step averaging. Kinesin steps were automatically isolated from the data by using a running *t*-test algorithm. For each data point, *W* (ms) of samples before and after that sample were compared by *t*-test. For positive force traces, *W* was 8 ms. In the faster assisting-force records, *W* was 6 ms. The resulting *t*-profile shows upward spikes for forward steps and downward spikes for backward steps (and for releases at positive forces).

Absolute *t*-values above a defined threshold were scored as steps, and the peak value was defined as time zero for their corresponding steps. An upper step-size limit of 12 nm was applied, to remove detachments and a small number of very fast double steps from consideration.

The dwell time is the time between steps. For a dwell time to be scored, both the current step and the preceding step had to fit the criteria above. We also required that the end position of the preceding step must not be more than 5 nm from the start position of the current step. This reduced the chance of erroneously scoring long dwells where steps were not resolved. We excluded steps that occurred in the range −1 to 1 pN because of the high positional noise in this region. At forces at which both forward and backward steps occurred (5–8 pN), the dwell time distribution for forward steps was distorted by the occurrence of backward steps, and vice versa.

For step averaging, further refinement of step position was performed by fitting exponentials to the steps identified by the *t*-test. In an iterative routine, the time constant that gave the minimum least-sums-of-squares fit to complete data series (typically 50–200 steps) was used to refine the step positions. For ensemble averaging, all steps were brought into register by using time zero for the fitted exponential.

Received 13 December 2004; accepted 9 March 2005.

1. Kaseda, K., Higuchi, H. & Hirose, K. Alternate fast and slow stepping of a heterodimeric kinesin molecule. *Nature Cell Biol.* **5,** 1079–1082 (2003).
2. Asbury, C. L., Fehr, A. N. & Block, S. M. Kinesin moves by an asymmetric hand-over-hand mechanism. *Science* **302,** 2130–2134 (2003).
3. Yildiz, A., Tomishige, M., Vale, R. D. & Selvin, P. R. Kinesin walks hand-over-hand. *Science* **303,** 676–678 (2004).
4. Svoboda, K., Schmidt, C. F., Schnapp, B. J. & Block, S. M. Direct observation of kinesin stepping by optical trapping interferometry. *Nature* **365,** 721–727 (1993).
5. Kojima, H., Muto, E., Higuchi, H. & Yanagida, T. Mechanics of single kinesin molecules measured by optical trapping nanometry. *Biophys. J.* **73,** 2012–2022 (1997).
6. Coppin, C. M., Finer, J. T., Spudich, J. A. & Vale, R. D. Detection of sub-8-nm movements of kinesin by high-resolution optical-trap microscopy. *Proc. Natl Acad. Sci. USA* **93,** 1913–1917 (1996).
7. Nishiyama, M., Muto, E., Inoue, Y., Yanagida, T. & Higuchi, H. Substeps within the 8-nm step of the ATPase cycle of single kinesin molecules. *Nature Cell Biol.* **3,** 425–428 (2001).
8. Hua, W., Young, E. C., Fleming, M. L. & Gelles, J. Coupling of kinesin steps to ATP hydrolysis. *Nature* **388,** 390–393 (1997).
9. Schnitzer, M. J. & Block, S. M. Kinesin hydrolyses one ATP per 8-nm step. *Nature* **388,** 386–390 (1997).
10. Coy, D. L., Wagenbach, M. & Howard, J. Kinesin takes one 8-nm step for each ATP that it hydrolyzes. *J. Biol. Chem.* **274,** 3667–3671 (1999).
11. Visscher, K., Schnitzer, M. J. & Block, S. M. Single kinesin molecules studied with a molecular force clamp. *Nature* **400,** 184–189 (1999).
12. Hackney, D. D. Evidence for alternating head catalysis by kinesin during microtubule-stimulated ATP hydrolysis. *Proc. Natl Acad. Sci. USA* **91,** 6865–6869 (1994).
13. Cross, R. A. The kinetic mechanism of kinesin. *Trends Biochem. Sci.* **29,** 301–309 (2004).
14. Tsiavaliaris, G., Fujita-Becker, S. & Manstein, D. J. Molecular engineering of a backwards-moving myosin motor. *Nature* **427,** 558–561 (2004).
15. Reconditi, M. *et al.* The myosin motor in muscle generates a smaller and slower working stroke at higher load. *Nature* **428,** 578–581 (2004).
16. Rice, S. *et al.* A structural change in the kinesin motor protein that drives motility. *Nature* **402,** 778–784 (1999).
17. Nishiyama, M., Higuchi, H. & Yanagida, T. Chemomechanical coupling of the forward and backward steps of single kinesin molecules. *Nature Cell Biol.* **4,** 790–797 (2002).
18. Okada, Y., Higuchi, H. & Hirokawa, N. Processivity of the single-headed kinesin KIF1A through biased binding to tubulin. *Nature* **424,** 574–577 (2003).
19. Block, S. M., Goldstein, L. S. & Schnapp, B. J. Bead movement by single kinesin molecules studied with optical tweezers. *Nature* **348,** 348–352 (1990).
20. Hunt, A. J., Gittes, F. & Howard, J. The force exerted by a single kinesin molecule against a viscous load. *Biophys. J.* **67,** 766–781 (1994).
21. Svoboda, K. & Block, S. M. Force and velocity measured for single kinesin molecules. *Cell* **77,** 773–784 (1994).
22. Kawaguchi, K. & Ishiwata, S. Temperature dependence of force, velocity, and processivity of single kinesin molecules. *Biochem. Biophys. Res. Commun.* **272,** 895–899 (2000).
23. Kramers, H. A. Brownian motion in a field of force and the diffusion limit of chemical reactions. *Physica* **7,** 284–304 (1940).
24. Nishiyama, M., Higuchi, H., Ishii, Y., Taniguchi, Y. & Yanagida, T. Single molecule processes on the stepwise movement of ATP-driven molecular motors. *Biosystems* **71,** 145–156 (2003).
25. Howard, J. *Mechanics of Motor Proteins and the Cytoskeleton* (Sinauer, Sunderland, Massachusetts, 2001).
26. Coppin, C. M., Pierce, D. W., Hsu, L. & Vale, R. D. The load dependence of kinesin's mechanical cycle. *Proc. Natl Acad. Sci. USA* **94,** 8539–8544 (1997).
27. Hirose, K., Lockhart, A., Cross, R. A. & Amos, L. A. Three-dimensional cryoelectron microscopy of dimeric kinesin and ncd motor domains on microtubules. *Proc. Natl Acad. Sci. USA* **93,** 9539–9544 (1996).
28. Schief, W. R. & Howard, J. Conformational changes during kinesin motility. *Curr. Opin. Cell Biol.* **13,** 19–28 (2001).
29. Rice, S. *et al.* Thermodynamic properties of the Kinesin neck-region docking to the catalytic core. *Biophys. J.* **84,** 1844–1854 (2003).
30. Schnitzer, M. J., Visscher, K. & Block, S. M. Force production by single kinesin motors. *Nature Cell Biol.* **2,** 718–723 (2000).
31. Fisher, M. E. & Kolomeisky, A. B. Simple mechanochemistry describes the dynamics of kinesin molecules. *Proc. Natl Acad. Sci. USA* **98,** 7748–7753 (2001).
32. Thomas, N., Imafuku, Y., Kamiya, T. & Tawada, K. Kinesin: a molecular motor with a spring in its step. *Proc. R. Soc. Lond. B* **269,** 2363–2371 (2002).
33. Block, S. M., Asbury, C. L., Shaevitz, J. W. & Lang, M. J. Probing the kinesin reaction cycle with a 2D optical force clamp. *Proc. Natl Acad. Sci. USA* **100,** 2351–2356 (2003).
34. Huxley, A. F. Muscle structure and theories of contraction. *Prog. Biophys. Biophys. Chem.* **7,** 257–318 (1957).
35. Huxley, A. F. & Simmons, R. M. Proposed mechanism of force generation in striated muscle. *Nature* **233,** 533–538 (1971).

Supplementary Information is linked to the online version of the paper at www.nature.com/nature.

Acknowledgements We thank J. Howard for the gift of the *Drososphila* kinesin, the reviewers of this manuscript for careful and constructive criticism, and Marie Curie Cancer Care for unswerving support.

Author Information Reprints and permissions information is available at npg.nature.com/reprintsandpermissions. The authors declare no competing financial interests. Correspondence and requests for materials should be addressed to R.A.C. (r.cross@mcri.ac.uk).